Available online at www.sciencedirect.com
SCIENCE DIRECT
Journal of Solid State Chemistry 173 (2003) 203–208
JOURNAL OF SOLID STATE CHEMISTRY
http://elsevier.com/locate/jssc

$Sr_{18}Ru_{1.9}Bi_{4.1}O_{33}$: crystallization of a Ru(V)/Bi(V) oxide from molten hydroxide

Marisol S. Martín-González, James L. Delattre, and Angelica M. Stacy*

Department of Chemistry, University of California at Berkeley, 538A Latimer, Berkeley, CA 94720, USA

Received 7 March 2002; received in revised form 22 November 2002; accepted 11 December 2002

Abstract

Single crystals of a new complex oxide, $Sr_{18}Ru_{1.9}Bi_{4.1}O_{33}$, were precipitated from a mixture of molten alkali and alkaline earth metal hydroxides at 750°C. The structure was determined from a ruby-red crystal using single-crystal X-ray diffraction. $Sr_{18}Ru_{1.88}Bi_{4.12}O_{33}$ crystallizes in the space group *C2/c* (monoclinic) and has unit-cell dimensions: $a = 10.2102(11)$ Å, $b = 17.882(2)$ Å, $c = 19.579(2)$ Å, and $\beta = 102.043(2)°$. The structure (refined to $R_1 = 4.5\%$, $wR_2 = 9.2\%$) is an unusual ABO_3 defect perovskite, with $\frac{1}{12}$th of the oxygen positions vacant. All the A sites and half of the B sites are occupied by Sr^{2+}, while the remaining B sites are occupied by Bi^{5+} or Ru^{5+}. The oxygen atom vacancies are located within the Bi coordination sphere exclusively. The bonding in the BO_3 sublattice is less covalent than that in the perovskite archetype from which it is derived due to the presence of 50% Sr^{2+} on the B sites. Thus, the structure of $Sr_{18}Ru_{1.9}Bi_{4.1}O_{33}$ can also be viewed as being made up of isolated bismuthate anions (BiO_5^{5-}, $BiO_{5.5}^{6-}$ and BiO_6^{7-}) and ruthenate anions (RuO_6^{7-}) separated by strontium cations.

Keywords: Molten hydroxide; Ruthenates; Bismuthates; Perovskites; Cryolite; Elpasolite

1. Introduction

The perovskite structure constitutes one of the most interesting structures in solid-state chemistry and continues to be investigated as a model for the study of fundamental properties in structural chemistry and physics. This is partly due to the extensive range of phase transitions that can be induced by composition changes, temperature, or pressure. The structure is known with the ABX_3 formula, where BX_6 octahedra are connected by corner-sharing X atoms in a three-dimensional framework with the A cations occupying positions coordinated by 12 X atoms. One of the many possible superstructures that can be derived from this framework [1] is cryolite (A_3BX_6) [2]. This superstructure can also be written from the structural standpoint as $A_2(A'B)X_6$. The cation A occupies two sites in the cryolite structure: all the A positions of the perovskite structure with coordination number (CN) = 12 plus half of the BX_6 positions with CN = 6. The framework is then constructed from $A'X_6$ and BX_6 octahedra connected by corners. This cryolite structure can also be considered as part of the elpasolite family ($A_2BB'X_6$) if A and B are the same cation [1,3,4]. Most of the cryolite-type compounds are halides [5], although oxides like R_3WO_6, R_3MoO_6 [6], $Ca_5Nb_2TiO_{12}$ [7], $Ca_4Nb_2O_9$ [8,9], or $Sr_3(Sr_{1+x}Nb_{2-x})O_{9-3/2x}$ [10] have been prepared. In the case of $Sr_3(Sr_{1+x}Nb_{2-x})O_{9-3/2x}$, the structure forms with up to 8.3% oxygen vacancies which corresponds to a limiting composition of $x = 0.5$ ($Sr_6Nb_2O_{11}$) [10]. We report here the properties of an oxygen-deficient mixed-metal (Ru^{5+}, Bi^{5+}) perovskite, $Sr_{18}Ru_{1.9}Bi_{4.1}O_{33}$, which is related to the cryolite archetype.

$Sr_{18}Ru_{1.9}Bi_{4.1}O_{33}$ was prepared from a molten KOH-$Sr(OH)_2$ flux and structurally characterized using single-crystal X-ray diffraction. The use of molten hydroxides provides a highly oxidizing environment at moderate temperatures and offers a synthetic route to complex transition metal oxides. The materials that have been obtained by this method are sometimes metastable and often contain transition metals in unusual or elevated oxidation states as exemplified by Ni^{4+} in $Ba_6Ni_5O_{15}$ [11], Bi^{5+} in Ba_3NaBiO_6 [12], Rh^{5+} in Sr_3NaRhO_6 [13], or Os^{7+} in Ba_2MOsO_6 (M = Li, Na) [14]. As described

*Corresponding author. Fax: +1-510-642-8369.
E-mail address: stacy@cchem.berkeley.edu (A.M. Stacy).

doi:10.1016/S0022-4596(03)00025-2

further below, $Sr_{18}Ru_{1.9}Bi_{4.1}O_{33}$ is an oxygen-deficient mixed-metal perovskite with Ru^{5+} and Bi^{5+}.

2. Experimental

The synthesis of $Sr_{18}Ru_{1.9}Bi_{4.1}O_{33}$ was carried out by adding 0.025 g RuO_2 (Alfa Aesar, 99.95%), 0.0909 g $Sr(OH)_2$ (obtained from Alfa Aesar, ultrapure, $Sr(OH)_2 \cdot 8H_2O$ dehydrated at 350°C), 0.0429 g Bi_2O_3 (Aldrich, 99.9%), and 2 g of KOH (Fisher, 85.8%) into a 5 ml alumina crucible, which was capped with an alumina lid. The crucible was placed in a furnace and heated at room temperature to 750°C in 6 h, then soaked at 750°C for another 6 h, and finally cooled to 600°C over the course of 48 h. During the heating process, a fraction of the molten flux sealed the lid tightly to the crucible. Upon removing the lid, ruby-red crystals were found at the bottom of the crucible. Single crystals were isolated by hand in an anaerobic box, since they are not stable under ambient conditions.

Single crystals were coated in Paratone-N oil, attached to quartz fibers, transferred to a Bruker SMART CCD area detector diffractometer, and cooled in a N_2 stream, $T = -149$°C. A face-indexed absorption correction was applied to the integrated and merged data, and a spherical absorption correction was applied using Multiscan [15]. The heavy atoms were located using direct methods [16]. As the refinement progressed it became apparent that the oxygen atoms around Bi3 were disordered. The disorder was modeled as two superimposed BiO_5^{5-} anions that are related by two-fold rotational symmetry. The site occupancy factors (SOFs) for the oxygen atoms coordinated to Bi3 summed to 5. The thermal parameter for O8, which is coordinated to Bi2, was very large relative to the thermal parameters for the rest of the oxygen atoms. The SOF for O8 was refined to 0.52, and then was fixed at 0.5 for subsequent refinements. Next, the strontium, bismuth, and ruthenium atoms were refined anisotropically. At this point, the thermal parameters on the ruthenium atoms were very small relative to all others, so the ruthenium sites were refined for partial substitution with bismuth. Refinement of the partial substitution gave 7% bismuth on the Ru1 site and 5% bismuth on the Ru2 site. The final cycle of full-matrix least-squares refinement against F^2 was based on 2962 unique reflections and 193 variable parameters. Crystal data are given in Table 1. Atomic coordinates and SOFs are listed in Table 2.

Table 1
Crystal data and structure refinement for $Sr_{18}Ru_{1.9}Bi_{4.1}O_{33}$

Empirical formula	$Sr_{36}Ru_{3.8}Bi_{8.2}O_{66}$
Formula weight	6313.42
Temperature	143(2) K
Wavelength	0.71073 Å
Crystal system, space group	Monoclinic, $C2/c$
Unit-cell dimensions	$a = 10.2102(11)$ Å $\alpha = 90°$ $b = 17.882(2)$ Å $\beta = 102.043(2)°$ $c = 19.579(2)$ Å $\gamma = 90°$
Volume	3496.2(7) $Å^3$
Z, calculated density	2, 5.997 g cm^{-3}
Absorption coefficient	48.759 mm^{-1}
$F(000)$	5492
Crystal size	$0.080 \times 0.060 \times 0.055$ mm^3
Theta range for data collection	2.13–25.55°
Limiting indices	$-12 \leqslant h \leqslant 11$, $-14 \leqslant k \leqslant 21$, $-22 \leqslant l \leqslant 23$
Reflections collected/unique	7737/2962 [$R_{(int)} = 0.0870$]
Completeness to theta = 25.55	90.1%
Refinement method	Full-matrix least-squares on F^2
Data/restraints/parameters	2962/0/193
Goodness-of-fit on F^2	0.993
Final R indices [$I > 2\sum(I)$]	$R_1 = 0.0448$, w$R_2 = 0.0917$
R indices (all data)	$R_1 = 0.0796$, w$R_2 = 0.0992$
Largest diff. peak/hole	1.873/−2.704e^- $Å^{-1}$

Table 2
Atomic coordinates ($\times 10^4$), equivalent isotropic displacement parameters ($Å^2 \times 10^3$) and site occupancy factors for $Sr_{18}Ru_{1.9}Bi_{4.1}O_{33}$. $U_{(eq)}$ is defined as one-third of the trace of the orthogonalized U_{ij} tensor

Atom	x	y	z	$U_{(eq)}$	SOF
Bi(1)	0	5635(1)	7500	18(1)	0.5
Bi(2)	7325(1)	4218(1)	4996(1)	16(1)	1
Bi(3)	5000	7308(1)	7500	23(1)	0.5
Sr(1)	6146(2)	5669(1)	6157(1)	24(1)	1
Sr(2)	10,748(2)	4180(1)	6240(1)	20(1)	1
Sr(3)	8458(2)	2895(1)	3743(1)	30(1)	1
Sr(4)	13,313(2)	5422(1)	6905(1)	21(1)	1
Sr(5)	9669(2)	2438(1)	5462(1)	17(1)	1
Sr(6)	1029(2)	4041(1)	4464(1)	18(1)	1
Sr(7)	3113(2)	2523(1)	6748(1)	20(1)	1
Sr(8)	5759(2)	3889(1)	9225(1)	17(1)	1
Sr(9)	7689(2)	3874(1)	6864(1)	19(1)	1
Ru(1)	5000	3913(1)	7500	13(1)	0.461(4)
Bi(4)	5000	3913(1)	7500	13(1)	0.038(4)
Ru(2)	2500	2500	5000	14(1)	0.478(4)
Bi(5)	2500	2500	5000	14(1)	0.021(4)
O(1)	1902(11)	3193(6)	5624(6)	14(3)	1
O(2)	6746(11)	6670(6)	5453(6)	15(3)	1
O(3)	791(11)	2611(6)	4341(6)	13(3)	1
O(4)	5487(12)	3138(7)	6905(7)	23(3)	1
O(5)	3122(12)	3979(7)	6961(6)	18(3)	1
O(6)	5514(11)	4683(6)	6877(6)	14(3)	1
O(7)	6289(13)	3725(7)	4069(7)	28(3)	1
O(8)	5380(20)	4829(14)	5001(14)	20(6)	0.5
O(9)	9115(13)	3710(7)	4999(7)	27(3)	1
O(10)	7712(13)	5174(7)	4458(7)	25(3)	1
O(11)	8071(12)	4764(7)	5937(6)	22(3)	1
O(12)	6625(12)	3353(7)	5579(7)	26(3)	1
O(13)	8401(16)	6141(9)	6902(8)	52(5)	1
O(14)	0	4458(11)	7500	30(5)	0.5
O(15)	873(14)	5677(8)	6614(8)	38(4)	1
O(16)	5290(30)	7941(14)	6664(13)	41(7)	0.6
O(17)	4390(40)	7940(20)	6610(20)	51(11)	0.4
O(18)	3090(20)	7544(13)	7285(13)	35(6)	0.6
O(19)	3020(50)	6890(30)	7400(30)	90(17)	0.4
O(20)	5420(30)	6240(16)	7318(16)	45(8)	0.5

3. Results and discussion

The crystal structure of $Sr_{18}Ru_{1.9}Bi_{4.1}O_{33}$ can be described from two different viewpoints. It can be considered as *condensed* (as a superstructure related to the perovskites $SrBiO_3$ [17] and $SrRuO_3$ [18]), or it can be viewed as an *isolated anionic structure* (as an assemblage of isolated ruthenate and bismuthate polyhedra).

From the condensed view, $Sr_{18}Ru_{1.9}Bi_{4.1}O_{33}$ can be considered an aggregate of 12 ABO_3 units to give an $A_{12}B_{12}O_{36}$ superstructure. The relationship is more clear if the empirical formula is rewritten as $Sr_{12}(Sr_6Ru_{1.9}Bi_{4.1})O_{36-\delta}$ with $\delta = 3$. The three oxygen vacancies are not random, but are confined to the Bi^{5+} coordination spheres. All of the *A* sites and half of the *B* sites are occupied by Sr, namely Sr1, Sr2, and Sr3. Bismuth and ruthenium atoms occupy the remaining *B* sites. This distribution is characteristic of the cryolite family [2].

The relationship between this structure and the cubic perovskite structure can be demonstrated by showing that the unit-cell parameters of this material can be explained in terms of a "supercell" derived from a small cubic unit cell. First, consider a cubic perovskite unit cell "*A*" with lattice parameter $a = 4.2$ Å (calculated by using the Bi^{5+}–O distance in $SrBiO_3$ [17]). If the unit cell "*A*" is transformed according to the matrix *M*:

$$M = \begin{bmatrix} 2 & -1 & -1 \\ 0 & 3 & -3 \\ 2 & 3 & 3 \end{bmatrix},$$

a second unit cell "*B*" is obtained with lattice parameters that are remarkably similar to the lattice parameters observed for $Sr_{12}(Sr_6Ru_{1.88}Bi_{4.12})O_{36-3}$ (see Table 3).

A view of the polyhedra that occupy the (202) lattice plane is shown in Fig. 1a. This view also corresponds to the (100) lattice plane of the cubic perovskite subunit. RuO_6 units are shown as black octahedra, BiO_x units are shown as gray polyhedra and SrO_x units are shown as ball and stick representations. For clarity, only the Sr atoms that occupy the perovskite B positions are shown.

Table 3
Comparison of lattice parameters for $Sr_{12}(Sr_6Ru_{1.88}Bi_{4.12})O_{36-\delta}$ vs. a calculated unit cell ("*b*")

Parameter	$Sr_{12}(Sr_6Ru_{1.88}Bi_{4.12})O_{36-3}$	Calc. "*b*"
a (Å)	10.2102(11)	10.29
b (Å)	17.882(2)	17.82
c (Å)	19.579(2)	19.70
α (Å)	90.00	90.00
β (°)	102.043(2)	100.02
γ (°)	90.00	90.00
Vol. (Å^3)	3496.2(7)	3557.2

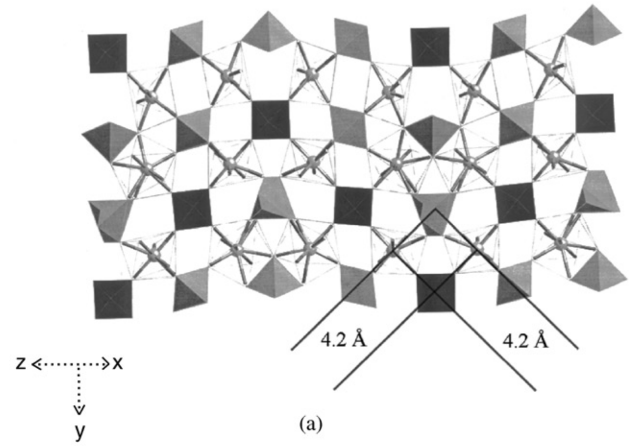

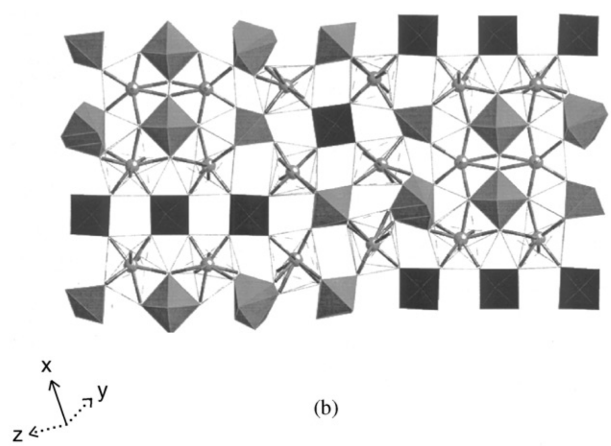

Fig. 1. Crystal structure of $Sr_{18}Ru_{1.9}Bi_{4.1}O_{33}$ (a) viewed along the [202] direction and (b) viewed along the [$\bar{1}$33]; which corresponds to the (100) and (010) planes of the perovskite subunit. The 4.2×4.2 Å^2 face of the perovskite subunit is shown in Fig. 1a in order to make clear the relationship between the layer and the cubic subcell. Strontium atoms occupy all of the perovskite *A* sites (not shown) and half of the *B* sites, which are shown as ball and stick representations. Bi^{5+} and Ru^{5+} occupy the remaining *B* sites. BiO_5^{5-}, $BiO_{5.5}^{6-}$ and BiO_6^{7-} anions are shown as gray polyhedra, while RuO_6^{7-} units are shown as black octahedra. A unit cell of the cubic perovskite (lattice parameter = 4.2 Å) from which this superstructure is derived is framed with black lines. Ruthenate polyhedra are shown as dark gray, bismuthate polyhedra as light gray, and strontium atoms on *B* sites are shown in white.

The prominent feature in the (202) plane is the inclusion of Sr atoms on every other B site. This ordering isolates the Ru and Bi atoms from one another, preventing any Ru–O–Ru, Ru–O–Bi or Bi–O–Bi bonding sequences. The RuO_6 octahedra are arranged in a zigzag pattern that stacks in the *b* direction. The zigzag chain is composed of linear Ru–O–Sr–O–Ru units that repeat twice for each segment of the chain.

The ($\bar{1}$33) plane, shown in Fig. 1b, coincides with the (010) plane of the perovskite subunit. This lattice plane also consists of ordered Sr atoms on every other B site. Here the Ru atoms lie in a 3:1:3:1 stepped pattern with each set of steps stacking on top of another set. The perovskite (001) plane, which corresponds to the ($\bar{1}\bar{3}3$) plane of the monoclinic lattice, is symmetry related to the (010) plane by a two-fold rotation axis that coincides with the b lattice vector in the monoclinic lattice. Hence, the connectivity within these two normal planes is the same.

An analysis of the oxidation states is consistent with the formulation that three out of every 36 oxygen atom positions of the perovskite "supercell" are vacant. Since Sr^{2+} occupies half of the B sites in the ABO_3 perovskite structure, if all 36 oxygen atoms were present then the oxidation states of the other metal atoms on the B sites would be 6+. With three out of 36 oxygen vacancies, the Bi and Ru oxidation states are 5+. As discussed further below, the oxygen vacancies are associated exclusively with the coordination sphere of the Bi atoms. Because of the oxygen vacancies and the substitution of Sr^{2+} onto the B sites, the structure is clearly more complex than the cubic perovskite structure of $ABiO_3$. It is interesting to notice that three out of 36 corresponds to ~8.3% oxygen vacancies, which is exactly the maximum value observed for the $Sr_3(Sr_{1+x}Nb_{2-x})O_{9-3/2x}$ solid solution for $x = 0.5$ [10].

From an isolated anionic structure approach, $Sr_{18}Ru_{1.9}Bi_{4.1}O_{33}$ can be viewed as being comprised of isolated bismuthate anions (BiO_5^{5-}, $BiO_{5.5}^{6-}$ and BiO_6^{7-}) and ruthenate anions (RuO_6^{7-}) with interstitial strontium cations. A list of bond distances and angles are given in Table 4.

A number of structures containing Bi in the high oxidation state of 5+ have been described in the literature [19,20]. In all of these cases, bismuth is octahedrally coordinated with Bi^{5+}–O distances ranging from 2.00 to 2.17 Å. No vacancies have been found in the BiO_6 octahedra except for the $Li_2Ba_5Bi_2O_{11}$ in which distorted BiO_6 octahedra are missing an oxygen atom 16% of the time [12]. In this compound, Bi1, shown in Fig. 2a, has Bi–O distances ranging from 2.02 to 2.11. There are five oxygen atoms surrounding Bi1 in an approximate trigonal–bipyramidal environment with an axial bond angle of 175.9° and equatorial bond angles that sum to 360°. The perfect planarity observed for the equatorial oxygen atoms is imposed by crystallography, as Bi1 and O14 occupy a two-fold rotation axis. This coordination geometry is quite reasonable in terms of valence bond theory popularized by Brown [21,22]. Using the published R_0 value for Bi^{5+} and O^{2-} of 2.06 Å [26], the valence bond sum for Bi1 is +4.89. Moreover, this geometry can also be found in compounds with Sb^{5+} or Pb^{4+} like in the cases of $Rb_5Sb_7TiO_{22}$ [23] or $K_2Li_6[Pb_2O_8]$ [24]. For Bi^{3+}, a pseudo-trigonal–bipyramidal coordination, with its lone-pair electrons occupying an equatorial position, can be found in β-Bi_2O_3 [25].

Bi2 has approximate square pyramidal coordination, as shown in Fig. 2b, but a sixth oxygen atom with 50% occupancy (O8) is located at 2.27 Å to give a partial pseudo-octahedral coordination. This bond distance is longer than the typical Bi^{5+}–O bond distances, which range from 2.04 to 2.17 Å. The oxygen atoms at the base of the square pyramid are tilted slightly toward the vacancy with an average bond angle between the apex

Table 4
Selected bond distances (Å) and angles (°) for $Sr_{18}Ru_{1.9}Bi_{4.1}O_{33}$

Bi(1)–O(13)	2.015(16)	(X2)
Bi(1)–O(14)	2.105(19)	
Bi(1)–O(15)	2.111(14)	(X2)
Bi(2)–O(9)	2.040(13)	
Bi(2)–O(11)	2.084(13)	
Bi(2)–O(10)	2.089(13)	
Bi(2)–O(7)	2.095(13)	
Bi(2)–O(12)	2.132(13)	
Bi(2)–O(8)	2.27(2)	
Bi(3)–O(18)	1.95(2)	(X2)
Bi(3)–O(20)	2.01(3)	(X2)
Bi(3)–O(16)	2.06(3)	(X2)
Bi(3)–O(17)	2.07(4)	(X2)
Bi(3)–O(19)	2.12(5)	(X2)
Ru(1)–O(4)	1.941(12)	(X2)
Ru(1)–O(6)	1.981(11)	(X2)
Ru(1)–O(5)	1.990(12)	(X2)
Ru(2)–O(1)	1.926(11)	(X2)
Ru(2)–O(3)	1.952(12)	(X2)
Ru(2)–O(2)	1.966(11)	(X2)
Sr(1)–O(2)	2.416(12)	
Sr(1)–O(6)	2.427(11)	
Sr(1)–O(13)	2.597(16)	
Sr(1)–O(8)	2.63(3)	
Sr(1)–O(11)	2.650(12)	
Sr(1)–O(7)	2.663(13)	
Sr(1)–O(8)	2.69(3)	
Sr(1)–O(20)	2.73(3)	
Sr(2)–O(16)	2.45(3)	
Sr(2)–O(1)	2.560(11)	
Sr(2)–O(10)	2.564(12)	
Sr(2)–O(5)	2.564(12)	
Sr(2)–O(15)	2.772(15)	
Sr(2)–O(9)	2.774(13)	
Sr(2)–O(14)	2.776(4)	
Sr(2)–O(17)	2.79(4)	
Sr(2)–O(11)	2.870(12)	
Sr(3)–O(18)	2.42(3)	
Sr(3)–O(19)	2.45(6)	
Sr(3)–O(3)	2.478(12)	
Sr(3)–O(4)	2.598(12)	
Sr(3)–O(12)	2.607(13)	
Sr(3)–O(15)	2.770(15)	
Sr(3)–O(9)	2.816(13)	
Sr(3)–O(7)	2.847(13)	
Sr(3)–O(17)	3.21(4)	

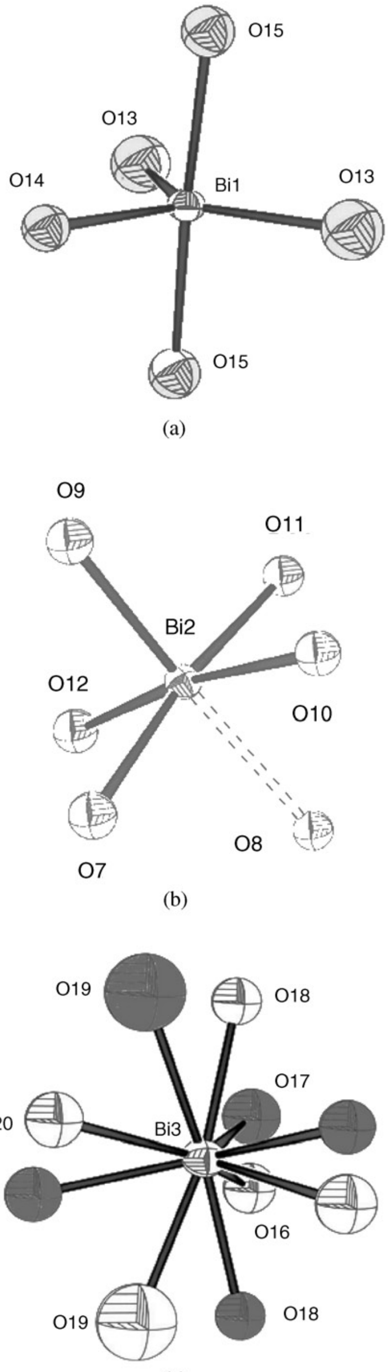

Fig. 2. ORTEP schematics of the bismuth–oxygen coordination polyhedra for: (a) trigonal–bipyramidal Bi1 (BiO_5^{5-}), (b) square pyramidal Bi2 with partial coordination to half-occupied O8 ($BiO_{5.5}^{6-}$), and (c) disordered trigonal–bipyramidal Bi3 (BiO_5^{5-}).

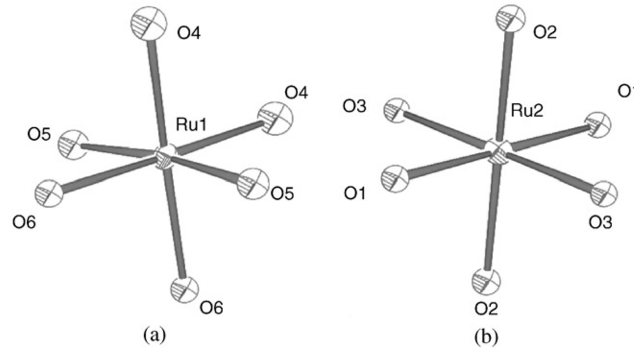

Fig. 3. ORTEP schematic of the ruthenium–oxygen coordination polyhedra of the ordered octahedra: (a) Ru1 and (b) Ru2.

oxygen atom (O9) and the base oxygen atoms (O7, O10, O11 and O12) of 94.7°.

This unusual coordination geometry can be validated with valence bond summations. The valence bond sum for Bi2 is +4.67, if O8 is excluded from the coordination sphere. In this case, Bi2 would be considered "under-bonded". If O8 is included in full occupancy, the valence bond sum for Bi2 is +5.27, which would be "over-bonded". However, if O8 is included in the coordination sphere with 50% occupancy, the valence bond sum for Bi2 is +4.97. This suggests that the $5+\frac{1}{2}$ coordination environment described is quite reasonable for Bi^{5+}. Thus, the valence bond analysis is consistent with the model of 50% occupancy determined from the refinement of crystallographic data.

The oxygen atoms around Bi3 are disordered but can be modeled as two partially occupied, distorted trigonal bipyramids that resemble the coordination environment of Bi1. Fig. 2c shows the two superimposed BiO_5^{5-} anions. The bond angle between axial oxygen atoms is 169.4° and the sum of the equatorial bond angles is 359.2°. The two partially occupied trigonal bipyramids are symmetry related to one another by a two-fold rotation axis that contains Bi3 but none of the oxygen atoms. The Bi3–O distance values range from 1.95 to 2.12 Å but due to the disorder, we were unable to extract useful bond valence sums. All the observed Bi^{5+}–O distances are in good agreement for what is found in others compounds [12,19,20,27–33].

In the case of perovskites with Ru^{5+}, like Sr_2ARuO_6 ($A = Y$, Eu ~ Lu) [34,35], Ba_2PrRuO_6 [36], or $Sr_4Ru_2O_9$ [37], Ru^{5+} is found typically in octahedral coordination, RuO_6, with Ru–O distances ranging from 1.888 to 1.96 Å. In our compound Ru1 and Ru2 have octahedral coordination (RuO_6^{7-}). Ru1 atoms have longer Ru–O distances ranging from 1.94 to 1.99 Å, whereas Ru2 atoms range from 1.93 to 1.97 Å (see ORTEP in Figs. 3a and b, respectively). The Ru^{5+}–O distances are similar to those reported for other Ru^{5+} oxides in which the Ru is surrounded by an octahedral array of O atoms (1.91–1.96 Å) [34–36]. A partial substitution of 7% bismuth can be found on the Ru1 site and 5% bismuth on the Ru2 site. Bi^{5+} in octahedral coordination has also been evidenced in other compounds like Bi_2O_4 [38], Bi_4O_7 [39], or Sr_2ScBiO_6 [40].

Bond valence summations for Ru1 and Ru2 have to be approached with some caution as the partial substitution of bismuth on these sites should have some effect on the average Ru–O distances. Still the calculated bond valence sums are quite reasonable, as the summations for Ru1 and Ru2 are +4.81 and +5.11, respectively. These summation values are based on the Ru^{5+}–O^{2-} bond valence parameter ($R_0 = 1.888$ Å) recently published by Dussarrat [37].

4. Conclusions

A new perovskite-related compound, $Sr_{18}Ru_{1.9}Bi_{4.1}O_{33}$, has been crystallized from a molten KOH-$Sr(OH)_2$ flux and the structure has been characterized by single-crystal X-ray diffraction. The structure can be described as *condensed* (as a superstructure related to the perovskites ABiO$_3$ and ARuO$_3$), or as an *isolated anionic structure* (as an assemblage of isolated ruthenate and bismuthate polyhedra). In terms of the ABO_3 perovskite structure, all the A sites and half of the B sites are occupied by Sr^{2+}, and either Bi^{5+} or Ru^{5+} occupies the remaining B sites with a small partial substitution of Bi^{5+} on some of the Ru^{5+} positions. From a molecular approach, the compound can be described as a collection of isolated bismuthate anions (BiO_5^{5-}, $BiO_{5.5}^{6-}$ and BiO_6^{7-}) and ruthenate anions (RuO_6^{7-}) interspersed with strontium cations. Bismuth and ruthenium both have oxidation states of 5+. The Bi^{5+} cations, which are usually octahedrally coordinated, display atypical five coordination.

Acknowledgments

A.M.S. thanks the Committee on Research at UC Berkeley for a Faculty Research Grant. M.S.M.G thanks MEC/Fulbright Fellowship program.

References

[1] C.N.R. Rao, J. Gopalakrishnan, K. Vidyasagar, Ind. J. Chem. 23A (1984) 265.
[2] A. Wells, Structural Inorganic Chemistry, 4th Edition, Clarendon Press, Oxford, 1975.
[3] K.S. Aleksandrov, V.V. Beznosikov, Phys. Solid State 39 (1997) 695–715.
[4] I.N. Flerov, M.V. Gorev, K.S. Aleksandrov, A. Tressaud, J. Grannec, M. Couzi, Mater. Sci. Eng. 24 (1998) 81–151.
[5] A. Bohnsack, G. Meyer, Z. Anorg. Allg. Chem. 622 (1996) 173–178.
[6] E.G. Steward, H.P. Rooksby, Acta Crystallogr. 4 (1951) 503.
[7] R.J. Cava, J.J. Krajewski, R.S. Roth, Mater. Res. Bull 34 (1999) 355.
[8] M. Hervieu, F. Studer, B.J. Raveau, Solid State Chem. 22 (1977) 273.
[9] I. Levin, L.A. Bendersky, J.P. Cline, R.S. Roth, T.A. Vanderah, J. Solid State Chem. 150 (2000) 43.
[10] J. Chan, I. Levin, T. Vanderah, R. Geyer, R. Roth, Int. J. Inorg. Mater. 2 (2000) 107–114.
[11] J.A. Campa, E. Gutierrez-Puebla, M.A. Monge, I. Raines, C.J. Ruiz-Valero, Solid State Chem. 108 (1994) 230.
[12] V. Carlson, A.M. Stacy, J. Solid State Chem. 96 (1992) 332–343.
[13] B.A. Reisner, A.M. Stacy, J. Am. Chem. Soc. 120 (1998) 9682.
[14] K.E. Stitzer, M.D. Smith, H.C. zur-Loye, Solid State Sci. 4 (2002) 311.
[15] R.H. Blessing, Acta Crystallogr. A 51 (1995) 33–38.
[16] G. Sheldrick, SHELX97, University of Göttingen, Germany, 1997.
[17] S.M. Kazakov, C. Chaillout, P. Bordet, J.J. Capponi, M. NunezRegueiro, A. Rysak, J.L. Tholence, P.G. Radaelli, S.N. Putilin, E.V. Antipov, Nature 390 (1997) 148–150.
[18] J.M. Longo, P.M. Raccah, J.B. Goodenough, J. Appl. Phys. 39 (1968) 1327–1328.
[19] F. Abbattista, C. Brisi, D. Mazza, M. Vallino, Mater. Res. Bull. 26 (1991) 107–117.
[20] A.M. Stacy, Abstr. Pap. Am. Chem. Soc. 205 (1993) 189.
[21] I.D. Brown, Chem. Soc. Rev 7 (1978) 359–376.
[22] I.D. Brown, Acta Crystallogr. B 41 (1985) 244–247.
[23] J. Almgren, G. Svensson, J. Albertsson, Acta Crystallogr. C 54 (1998) 1206.
[24] B. Brazel, R.Z. Hoppe, Anorg. Allg. Chem. 497 (1983) 176.
[25] S.K. Blower, C. Greaves, Acta Crystallogr. C 44 (1998) 587.
[26] N. Brese, M. O'Keeffe, Acta Crystallogr. B 47 (1991) 192–197.
[27] P.E. Kazin, A. Abakumov, D.D. Zaytsev, Y.D. Tretyakov, N.R. Khasanova, G.J. Van Tendeloo, Solid State Chem. 162 (2001) 142–147.
[28] E. Shuvaeva, E. Fesenko, Sov. Phys. Crystallogr. 14 (1970) 926.
[29] A. Lenz, H.J. Mullerbuschbaum, Less-Common Met. 16 (1990) 141–146.
[30] R. Horyn, M. Wolcyrz, A. Wojakowski, A. Zaleski, J. Alloys Compounds 242 (1996) 35–40.
[31] S. Blower, C. Greaves, Solid State Commun. 68 (1988) 765–767.
[32] J.L. Luce, A.M. Stacy, Chem. Mater. 9 (1997) 1508.
[33] T. Nguyen, D. Giaquinta, W. Davis, H. zur Loye, Chem. Mater. 5 (1993) 1273–1276.
[34] P. Battle, W.J. Macklin, Solid State Chem. 52 (1984) 138–145.
[35] Y. Doi, Y.J. Hinatsu, Phys.: Condens. Matter 11 (1999) 4813.
[36] Y. Izumiyama, Y. Doi, M. Wakeshima, Y. Hinatsu, Y. Shimojo, Y. Morii, J. Phys.: Condens. Matter 13 (2001) 1303–1313.
[37] C. Dussarrat, J. Fompeyrine, J. Darriet, Eur. J. Solid State Inorg. Chem. 32 (1995) 3–14.
[38] N. Kumada, N. Kinomura, P.M. Woodward, A.W. Sleight, J. Solid State Chem. 116 (1995) 217–433.
[39] R.E. Dinnebier, R.M. Ibberson, H. Ehrenberg, M. Jansen, J. Solid State Chem. 163 (2002) 332–339.
[40] P.E. Kazin, A.M. Abakumov, D.D. Zaytsev, Y.D. Tretyakov, N.R. Khasanova, G. Van Tendeloo, M. Jansen, J. Solid State Chem. 162 (2001) 142–147.